



Characterization of transient species produced from laser flash photolysis of a new cardioprotective drug: S-propargyl-cysteine

Kun Li^{a,1}, Hongbao Wang^{b,1}, Lingli Cheng^a, Mei Wang^a, Rongrong Zhu^a, Shi-Long Wang^{a,*}

^a School of Life Science and Technology, Tongji University, Shanghai City Siping Road 1239, Shanghai 200092, PR China

^b Department of Cardiology, Tongji Hospital, Tongji University, Shanghai 200065, PR China

ARTICLE INFO

Article history:

Received 14 September 2010

Received in revised form 31 January 2011

Accepted 17 February 2011

Available online 23 February 2011

Keywords:

Laser flash photolysis

S-propargyl-cysteine

Cardioprotective drug

Sulfur-containing amino acid

Antioxidant

ABSTRACT

S-propargyl-cysteine (SPRC), a sulfur-containing amino acid, was proved to have cardioprotective effect mediated by the CSE/H₂S pathway. In this study, photo-ionization of SPRC was investigated by 266 nm laser flash photolysis. Irradiated by 266 nm laser pulse, SPRC in aqueous solution experienced photo-ionization via a bi-photon process to produce hydrated electron, anion radical (SPRC^{•-}), and neutral radical (SPRC^{•(-H)}}). The reaction of SPRC with SPRC^{•-} was found and the pK_a of SPRC^{•+} was determined. Oxidation of SPRC by SO₄^{•-} not only confirmed the assignment of SPRC^{•(-H)}}, but also provided an evidence for the antioxidant activity of SPRC.

© 2011 Elsevier B.V. All rights reserved.

1. Introduction

Garlic is used traditionally as a complementary therapy in the treatment of several diseases such as diabetes, several forms of cancer, and neurodegenerative conditions [1,2]. A list of health-promoting and related biological effect has been ascribed to the organosulfur components of tissue preparations from garlic and onion [3]. S-allylcysteine (SAC), a sulfur-containing amino acid, is one of the major compounds in aged garlic extract [4]. SAC has been reported to have antioxidant activity [5,6], anti-cancer promoting activity [7–11], anti-hepatopathic activity [12,13], and neurotrophic activity [14,15]. Moreover, a recent study showed that the cardioprotective effect of SAC was associated with a hydrogen sulfide (H₂S)-mediated pathway in an acute myocardial infarction rat model (MI) [16]. SAC can undergo β-elimination and serve as the substrate of cystathionine-g-lyase (CSE) which is a pyridoxal-5-phosphate-dependent enzyme involved in endogenous hydrogen sulfide production [17]. Hydrogen sulfide might be the third endogenous signaling gasotransmitter, besides nitric oxide and carbon monoxide [18]. Hydrogen sulfide, at physiologically relevant concentrations, can alleviate myocardial ischemia-reperfusion injury [19–22].

S-propargyl-cysteine (SPRC) (Fig. 1), a structural analog of SAC, has the same cysteine-containing structure. Recent studies showed that SPRC had cardioprotective property in MI rats and preserved cell viability when cultured cells were exposed to hypoxia. Moreover, SPRC had better cardioprotective effect than SAC. The protective effect of SPRC was partly mediated by the CSE/H₂S pathway [23]. However, metabolism and pharmacology of SPRC have been ambiguously known by far. As we know, the pathogenesis of many cardio-vascular diseases is involved in the generation of active species such as ROS and nitrogen oxides. SPRC may react with these active species to produce many new transient species which may be associated with the metabolism of SPRC. Therefore, it is necessary to investigate these transient species resulting from SPRC in order to better understand the metabolism and pharmacology of SPRC.

In this work, laser flash photolysis (LFP) was employed to investigate photo-ionization of SPRC. Several new transient species produced from LFP have been identified. The antioxidant activity of SPRC was also proved by investigating reaction of SO₄^{•-} with SPRC. Meanwhile, a series of related kinetic parameters have been obtained.

2. Experimental

2.1. Chemical reagents

SPRC was kindly supplied by Prof. Yi Zhun Zhu (Department of Pharmacology, School of Pharmacy and Institute of Biomedical

* Corresponding author. Tel.: +86 21 65982595; fax: +86 21 65982286.

E-mail addresses: wsl@tongji.edu.cn, liangliang2419@126.com (S.-L. Wang).

¹ These authors contributed equally to this work.

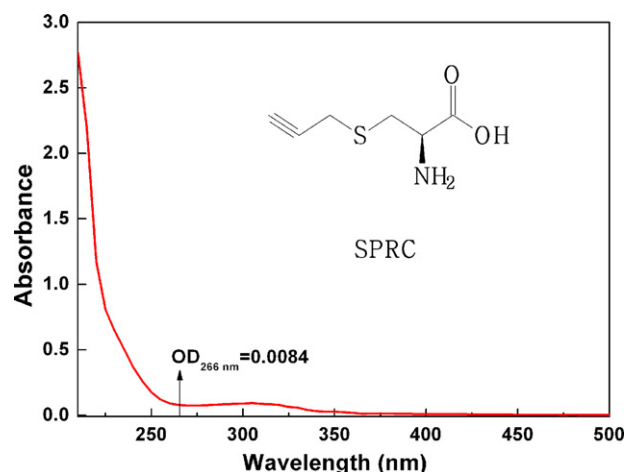


Fig. 1. The UV-vis spectrum of 5 mM SPRC aqueous solution at pH 6.7 and structural formula of SPRC.

Sciences, Fudan University, Shanghai, China) and used without further purification. Its purity ($\geq 99\%$) was checked by HPLC. Tert-Butyl alcohol (t-BuOH) and acetonitrile were purchased from Sigma. $K_2S_2O_8$, NaOH, $HClO_4$ and phosphate (analytic grade reagent) were commercially available and used without further purification. The pH value of the solution was adjusted by adding NaOH and $HClO_4$ solution. The solutions were deaerated with high-purity N_2 ($\geq 99.99\%$), N_2O , or O_2 ($\geq 99.5\%$) for different purposes by bubbling for at least 20 min prior to experiments. Ground-state absorption properties were studied by using a UV-vis spectrometer (VARIAN CARY 50 Probe). All experiments were performed in a 1 cm quartz cuvette at room temperature.

2.2. Laser flash photolysis experiments

Laser flash photolysis experiments were carried out by using Nd:YAG laser of 266 nm light pulses with a duration of 5 ns and the maximum energy of 40 mJ per pulse used as the pump light source. A xenon lamp was employed as detecting light source. The laser and analyzing light beam passed perpendicularly through a quartz cell with an optical path length of 10 mm. The transmitted light entered a monochromator equipped with an R955 photomultiplier. The output signal from the Agilent 54830B digital oscilloscope was transferred to a personal computer for data treatment. The LFP setup has been previously described [24–26].

3. Results and discussion

3.1. Characterization of photo-ionization of SPRC in aqueous solution

SPRC shows a very low absorption at 266 nm (Fig. 1). However, after 266 nm LFP of N_2 -saturated 5 mM SPRC aqueous solution, transient absorption spectra with two absorption bands centered at 300 and 330 nm and a strong and broad absorption band after 500 nm was obtained (Fig. 2). The transient species with the broad absorption band ($\lambda > 500$ nm) decayed fast. The kinetic decay curve observed at 700 nm can be efficiently quenched by N_2O with the addition of t-BuOH in the solution or O_2 (inset of Fig. 2). Therefore, it should be assigned to the hydrated electron (e_{aq}^-) [27,28]. The appearance of e_{aq}^- means that SPRC experienced photo-ionization to produce e_{aq}^- which can be captured by O_2 or N_2O (Eqs. (1)–(4)).

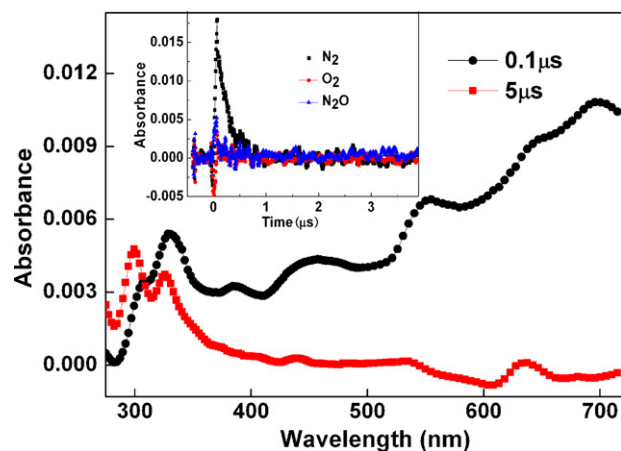
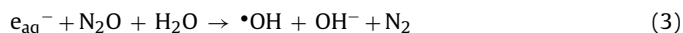


Fig. 2. Transient absorption spectra obtained from 266 nm LFP of N_2 -saturated 5 mM SPRC aqueous solution recorded at: (●) 0.1 μ s, (■) 5 μ s after laser pulse. Inset: kinetic decay curve observed at 700 nm saturated with (■) N_2 , (●) O_2 , and (▲) N_2O with t-BuOH, respectively.



In order to determine whether the photo-ionization of SPRC by 266 nm laser pulse is caused by a mono-photon or a bi-photon process, the yield of e_{aq}^- was calculated from OD_0 (optical density value recorded at 0 time after laser pulse) at 700 nm by changing intensity of laser pulse (I_L) [28]. For SPRC the yield of e_{aq}^- was found to increase with the square of the incident laser intensity (I_L) (Fig. 3). A $\log(OD_0)$ – $\log(I_L)$ plot yields slope of 1.8 (inset of Fig. 3). This clearly indicates that photo-ionization of SPRC proceeds in a two-photon process.

3.2. Reaction of SPRC with e_{aq}^-

Here, the decay of e_{aq}^- at 700 nm followed the pseudo-first-order kinetic process and was obviously accelerated with the increase of SPRC concentration (Fig. 4). This is ascribed predominantly to their reactions with the substrate molecules to form its radical anion ($SPRC^{\bullet-}$) (Eq. (5)). Since electrons are readily solvated in polar solvents, back electron transfer to the radical cation is not important [29,30]. The rate constant of reaction between SPRC and e_{aq}^- was determined to be $(5.32 \pm 0.10) \times 10^8 M^{-1} s^{-1}$ by monitoring the observed pseudo-first-order decay rate constant (k_{obs}) at

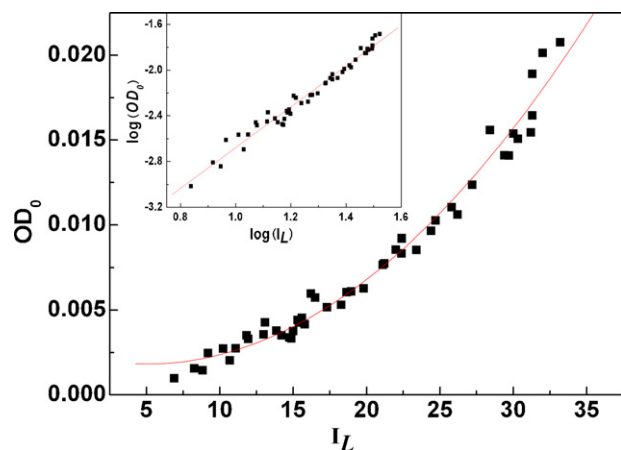


Fig. 3. Dependence of OD_0 at 700 nm on laser intensity (I_L) immediately after 266 nm LFP of N_2 -saturated 5 mM SPRC aqueous solution pH=6.7. Inset: plot of $\log(OD_0)$ vs $\log(I_L)$.

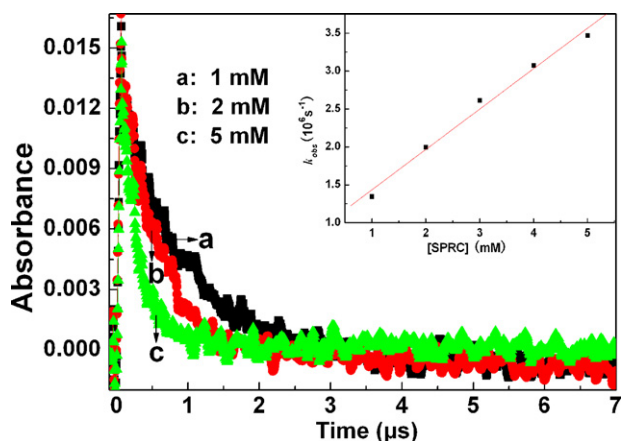


Fig. 4. Kinetic decay curve observed at 700 nm obtained from 266 nm LFP of N_2 -saturated aqueous solution pH = 6.7 containing different concentrations of SPRC: (a) 1 mM, (b) 2 mM and (c) 5 mM. Inset: plot of the observed pseudo-first-order decay rate constant (k_{obs}) at 700 nm vs SPRC concentration. The straight line represents a linear fit to the experimental data.

700 nm versus the SPRC concentration (inset of Fig. 4).



3.3. Reaction of SPRC with $SPRC^{\bullet-}$

The decay of e_{aq}^- is followed by the formation of an absorbance around 300 nm (Fig. 2). However, the buildup of 300 nm is not synchronous with the decay of e_{aq}^- at 700 nm (Fig. 5A). It suggested that the generated new transient species with absorption at 300 nm could not be ascribed to $SPRC^{\bullet-}$. The addition of e_{aq}^- scavengers,

such as O_2 and N_2O with t-BuOH, could eliminate the buildup trace at 300 nm (Fig. 5B), which implied that e_{aq}^- is indispensable for the buildup. Considering that $SPRC^{\bullet-}$ is the main initial product of the reaction of e_{aq}^- , the new species may result from the decay of $SPRC^{\bullet-}$. Then the kinetic analysis showed that the buildup process followed the pseudo-first-order kinetic process and the generation rate increased with a rate linearly proportional to the concentration of SPRC (Fig. 5C). Therefore, it could be inferred that SPRC involved in the formation of 300 nm. The new species could be ascribed to the product of the reaction of SPRC with $SPRC^{\bullet-}$ ($(2SPRC)^{\bullet-}$) (Eq. (6)). From a dependence of the observed generation rate (k_{obs}) on SPRC concentration (1–5 mM), the bimolecular rate can be estimated to be $(1.14 \pm 0.05) \times 10^8 M^{-1} s^{-1}$ (Fig. 5D).



3.4. Identification and the characterization of $SPRC^{\bullet-}(-H)$

SPRC was photo-ionized by 266 nm laser pulse irradiation to produce e_{aq}^- and the radical cation of SPRC ($SPRC^{\bullet+}$) or deprotonated radical cation of SPRC ($SPRC^{\bullet-}(-H)$). In order to confirm the absorption of $SPRC^{\bullet+}/SPRC^{\bullet-}(-H)$, transient absorption spectra was obtained from 266 nm LFP of O_2 -saturated 5 mM SPRC aqueous solution (Fig. 6). In this condition, O_2 can exclude the absorption of e_{aq}^- and products resulting from e_{aq}^- , or the potential triplet state of SPRC. The absorption band at 330 nm should be ascribed to $SPRC^{\bullet+}/SPRC^{\bullet-}(-H)$.

The transient absorption at 330 nm was investigated by changing pH value of the O_2 -saturated aqueous solution containing 5 mM SPRC (Fig. 7). According to the titration curve, the pKa value of $SPRC^{\bullet+}$ is obtained from the inflection point of the curve [31], which is 3.89. Given the pH value of SPRC solution is 6.7, $SPRC^{\bullet+}$ would

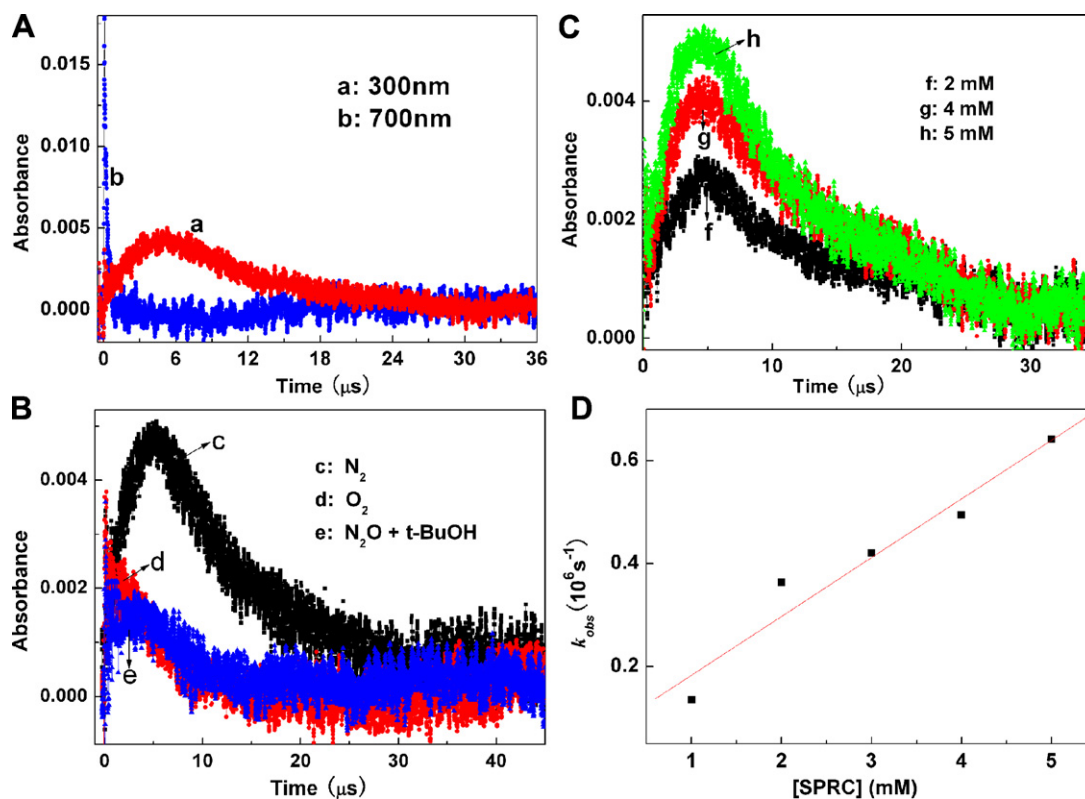


Fig. 5. (A) Kinetic decay curve obtained from 266 nm LFP of N_2 -saturated 5 mM SPRC aqueous solution observed at (a) 300 nm and (b) 700 nm, respectively. (B) Kinetic decay curve observed at 300 nm obtained from 266 nm LFP of 5 mM SPRC aqueous solution saturated with (c) N_2 or (d) O_2 or (e) N_2O with t-BuOH, respectively. (C) The buildup trace observed at 300 nm obtained from 266 nm LFP of N_2 -saturated aqueous solution containing different concentrations of SPRC: (f) 2 mM, (g) 4 mM and (h) 5 mM. (D) Plot of the observed generation rate constant k_{obs} at 300 nm vs SPRC concentration. The straight line represents a linear fit to the experimental data.

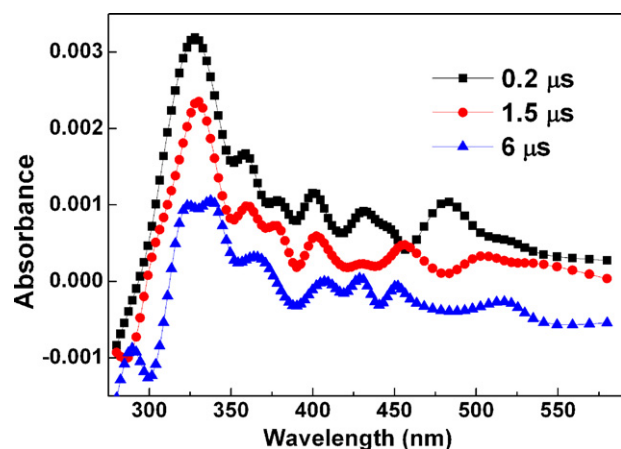


Fig. 6. Transient absorption spectra obtained from 266 nm LFP of O_2 -saturated 5 mM SPRC aqueous solution pH 6.7 recorded at: (■) 0.2 μ s, (●) 1.5 μ s, and (▲) 6 μ s after laser pulse.

change into $SPRC^*(-H)$ via deprotonation (Eq. (7)) and the absorption at 330 nm was attributed to $SPRC^*(-H)$.



3.5. Scavenging $SO_4^{\bullet-}$ by SPRC

SPRC may have antioxidant activity like other sulfur-containing amino acids. For the sake of gaining insight into the antioxidant activity of SPRC and further confirming the assignment of $SPRC^*(-H)$, the reaction of quenching $SO_4^{\bullet-}$ by SPRC was investigated. Concentration of $K_2S_2O_8$ (0.05 M OD=0.524) was designed to assure that $K_2S_2O_8$ absorbed the main energy of laser pulse and the absorption of SPRC (1 mM OD=0.0016) could be neglected. Fig. 8 shows that after the laser pulse, $SO_4^{\bullet-}$ with typical absorption around 450 nm was generated [32,33]. The decay of $SO_4^{\bullet-}$ was followed by the formation of new transient species with absorption around 330 nm. Transient absorption spectra showed the buildup trace of 330 nm was overlapped by the decay of $SO_4^{\bullet-}$. Here kinetic decay curve at 480 nm was chosen to represent the decay of $SO_4^{\bullet-}$ in order to avoid the disturbance of new transient species. According to the subtraction method [31], we have derived the pure growth trace at 330 nm which is synchronic with the decay of $SO_4^{\bullet-}$ at 480 nm (inset of Fig. 8). $SO_4^{\bullet-}$ can be generated easily by 266 nm LFP of $S_2O_8^{2-}$ (Eqs. (8) and (9)). As a one-electron oxidant, $SO_4^{\bullet-}$ can oxidize SPRC into $SPRC^{*+}$ which turns into $SPRC^*(-H)$ via deprotona-

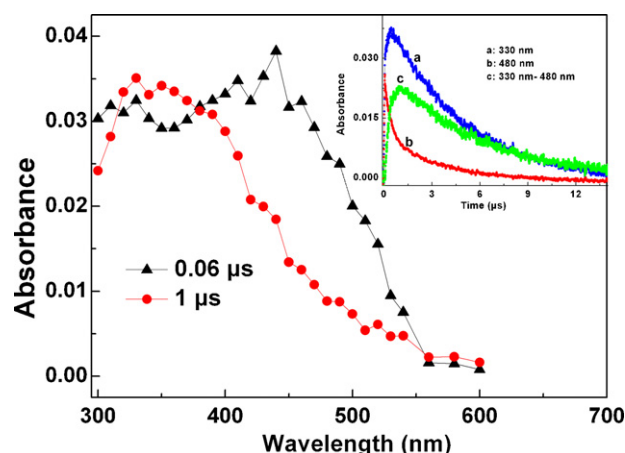


Fig. 8. Transient absorption spectra obtained from 266 nm LFP of N_2 -saturated aqueous solution pH 4.8 containing 1 mM SPRC and 0.05 M $K_2S_2O_8$ recorded at 0.06 μ s (▲) and 1 μ s (●) after laser pulse. Inset: kinetic decay curves at (a) 330 nm; (b) 480 nm; (c) the buildup trace of 330 nm obtained by subtracting trace (b) from trace (a).

tion (Eq. 7). Therefore, the new transient species could be assigned as $SPRC^*(-H)$. From a plot of the observed pseudo-first-order decay rate constant (k_{obs}) at 480 nm versus the SPRC concentration, the rate constant can be determined to be $(2.57 \pm 0.01) \times 10^9 M^{-1} s^{-1}$.



The rate constant shows that SPRC is very active to the strong oxidative radicals $SO_4^{\bullet-}$. Many heart diseases, such as myocardial ischemia-reperfusion injury and myocardial fibrogenesis, are associated with the generation of oxy-radical adducts (superoxide anion radical, $O_2^{\bullet-}$ and hydroxyl radicals, $\bullet OH$) or nitrogen oxides (peroxynitrite $NO_3^{\bullet-}$) [34–36]. Just like $SO_4^{\bullet-}$, $\bullet OH$ and $NO_3^{\bullet-}$ are also strong oxidative radicals. Considering the reaction of SPRC with $SO_4^{\bullet-}$, it can be inferred that $\bullet OH$ and $NO_3^{\bullet-}$ may be also easily eliminated by SPRC. SPRC was proposed to show cardioprotective effects partly mediated by the CSE/ H_2S pathway [23]. According to the ability of SPRC to eliminate strong oxidative radicals, another possible mechanism can be proposed that SPRC may show cardioprotective effects via directly scavenging the strong oxidative radicals (such as OH^{\bullet} and $NO_3^{\bullet-}$) generated in heart.

4. Conclusion

Photo-ionization of SPRC was investigated by 266 nm laser flash photolysis. The transient products of photo-ionization of SPRC were identified as e_{aq}^- , $SPRC^{\bullet-}$, $(2SPRC)^{\bullet-}$ and $SPRC^*(-H)$. The reactions of SPRC with e_{aq}^- , $SPRC^{\bullet-}$ and $SO_4^{\bullet-}$ were investigated. The results show that SPRC is a very active drug which cannot only be reduced by e_{aq}^- into $SPRC^{\bullet-}$ but also be oxidized by oxidative radical $SO_4^{\bullet-}$ into $SPRC^*(-H)$. e_{aq}^- can be easily generated by exposure of organism to sunlight and strong oxidative radicals (such as OH^{\bullet} and $NO_3^{\bullet-}$) are common active species in pathological tissues and organs. After absorbed by human body, SPRC inevitably reacts with these active species to produce new transient species, and thereby alleviates related diseases. Therefore, this study may be helpful to elucidate the pharmacology of SPRC.

Acknowledgements

The work was supported by the 973 project of the Ministry of Science and Technology (No. 2010CB912604 and 2010CB933901), Genetically modified organisms breeding major projects (No.

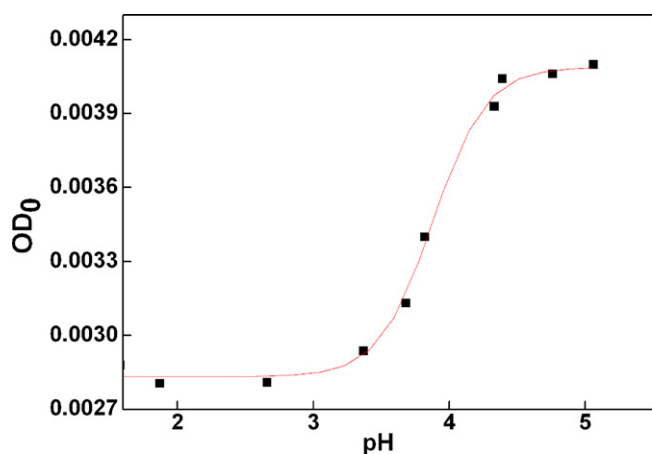


Fig. 7. Absorbance at 330 nm as a function of pH dependence, recorded immediately after the 266 nm laser pulse.

2009ZX08011-032B), and Shanghai key laboratory of cell signaling and diseases (Grant no 09DZ2260100).

References

- [1] S.K. Banerjee, S.K. Maulik, Effect of garlic on cardiovascular disorders: a review, *Nutr. J.* 1 (2002) 4–18.
- [2] K. Rahman, Garlic and aging: new insights into an old remedy, *Ageing Res. Rev.* 2 (2003) 39–56.
- [3] H. Xiao, L. Kirk, Parkin, Antioxidant functions of selected allium thiosulfonates and S-Alk(en)yl-L-Cysteine sulfoxides, *J. Agric. Food Chem.* 50 (2002) 2488–2493.
- [4] P. Rose, M. Whiteman, P.K. Moore, Y.Z. Zhu, Bioactive S-alk(en)yl cysteine sulfoxide metabolites in the genus *Allium*: the chemistry of potential therapeutic agents, *Nat. Prod. Rep.* 22 (2005) 351–368.
- [5] N. Ide, H. Benjamin, S. Lau, S-Allylcysteine attenuates oxidative stress in endothelial cells, *Drug Dev. Ind. Pharm.* 25 (1999) 619–624.
- [6] Y. Numagami, S.T. Ohnishi, S-Allylcysteine inhibits free radical production, lipid peroxidation and neuronal damage in rat brain ischemia, *J. Nutr.* 131 (2001) 1100–1105.
- [7] H. Sumiyoshi, M.J. Wargovich, Chemoprevention of 1,2-dimethyl hydrazine-induced colon cancer in mice by naturally occurring organo-sulfur compounds, *Cancer Res.* 50 (1990) 5084–5087.
- [8] Q.J. Chu, D.T.W. Lee, S.W. Tsao, X.H. Wang, Y.C. Wong, S-allylcysteine, a water-soluble garlic derivative, suppresses the growth of a human androgen-independent prostate cancer xenograft, CWR22R, under in vivo conditions, *BJU Int.* 99 (2006) 925–932.
- [9] C. Welch, L. Wuarin, N. Sidell, Antiproliferative effect of the garlic compound S-allylcysteine on human neuroblastoma cell in vitro, *Cancer Lett.* 63 (1992) 211–219.
- [10] H. Amagase, J.A. Milner, Impact of various sources of garlic and their constituents on 7,12-dimethyl-benz[α]anthracene binding to mammary cell DNA, *Carcinogenesis* 14 (1993) 1627–1631.
- [11] H. Takeyama, D.S.B. Hoon, R.E. Saxton, D.L. Morton, R.F. Irie, Growth inhibition and modulation of cell markers of melanoma by S-allylcysteine, *Oncology* 50 (1993) 63–69.
- [12] C.C. Hsu, C.C. Lin, T.S. Liao, M.C. Yin, Protective effect of S-allylcysteine and S-propyl cysteine on acetaminophen-induced hepatotoxicity in mice, *Food Chem. Toxicol.* 44 (2006) 393–397.
- [13] S. Nakagawa, S. Kasuga, H. Matsuura, Prevention of liver damage by aged garlic extract and its components in mice, *Phytother. Res.* 3 (1989) 50–53.
- [14] T. Moriguchi, H. Matsuura, Y. Koderu, Y. Itakura, H. Katsuki, H. Saito, N. Nishiyama, Neurotrophic activity of organosulfur compounds having a thioallyl group on cultured rat hippocampal neurons, *Neurochem. Res.* 22 (1997) 1449–1452.
- [15] N. Nishiyama, T. Moriguchi, N. Morihara, H. Saito, Ameliorative effect of S-allylcysteine, a major thioallyl constituent in aged garlic extract, on learning deficits in senescence accelerated mice, *J. Nutr.* 131 (2001) 1093–1095.
- [16] S.C. Chuah, P.K. Moore, Y.Z. Zhu, S-allylcysteine mediates cardioprotection in an acute myocardial infarction rat model via a hydrogen sulfide-mediated pathway, *Am. J. Physiol. Heart Circ. Physiol.* 293 (2007) 2693–2701.
- [17] J.T. Pinto, B.F. Krasnikov, A.J.L. Cooper, Redox-sensitive proteins are potential targets of garlic-derived mercaptocysteine derivatives, *J. Nutr.* 136 (2006) 835–841.
- [18] R. Wang, Two's company, three's a crowd: can H₂S be the third endogenous gaseous transmitter? *FASEB J.* 16 (2002) 1792–1798.
- [19] Y.Z. Zhu, Z.J. Wang, P.Y. Ho, Y.Y. Loke, Y.C. Zhu, X.W. Huang, S.H. Huang, C.S. Tan, M. Whiteman, J. Lu, P.K. Moore, Hydrogen sulfide and its cardioprotective effects in myocardial ischemia in experimental rats, *J. Appl. Physiol.* 102 (2007) 261–268.
- [20] J.W. Elrod, J.W. Calvert, J. Morrison, J.E. Doeller, D.W. Kraus, L. Tao, X.Y. Jiao, R. Scalia, L. Kiss, C. Szabo, H. Kimura, C.W. Chow, D.J. Lefer, Hydrogen sulfide attenuates myocardial ischemia-reperfusion injury by preservation of mitochondrial function, *PNAS* 104 (2007) 15560–15565.
- [21] B. Geng, L. Chang, C.S. Pan, Y.F. Qi, J. Zhao, Y.Z. Pang, J.B. Du, C.S. Tang, Endogenous hydrogen sulfide regulation of myocardial injury induced by isoproterenol, *Biochem. Biophys. Res. Commun.* 318 (2004) 756–763.
- [22] Y. Ji, Q.F. Pang, G. Xu, L. Wang, J.K. Wang, Y.M. Zeng, Exogenous hydrogen sulfide postconditioning protects isolated rat hearts against ischemia-reperfusion injury, *Eur. J. Pharmacol.* 587 (2008) 1–7.
- [23] Q. Wang, H.R. Liu, Q. Mu, P. Rose, Y.Z. Zhu, S-propargyl-cysteine protects both adult rat hearts and neonatal cardiomyocytes from ischemia/hypoxia injury: the contribution of the hydrogen sulfide-mediated pathway, *J. Cardiovasc. Pharmacol.* 54 (2009) 139–146.
- [24] L.L. Cheng, P. Zhao, M. Wang, H. Zhu, R.R. Zhu, X.Y. Sun, S.L. Wang, Photo-damage and photooxidation mechanisms of bovine serum albumin, *Acta Phys.-Chim. Sin.* 25 (2009) 25–29.
- [25] H. Zhu, M. Wang, L.L. Cheng, R.R. Zhu, X.Y. Sun, S.D. Yao, Q.S. Wu, S.L. Wang, Photoionization and photoexcitation mechanisms of salicylic acid, *Acta Phys.-Chim. Sin.* 26 (2010) 87–93.
- [26] M. Wang, L.L. Cheng, H. Zhu, K. Li, Q.S. Wu, S.D. Yao, S.L. Wang, Characterization of the transient species generated in the photoexcitation of benzoic acid, 2-hydroxy-, 2-d-ribofuranosylhydrazide, *J. Photochem. Photobiol. A: Chem.* 208 (2009) 104–109.
- [27] G.V. Buxton, C.L. Greenstock, W.P. Helman, A.B. Ross, Critical review of rate constants for reactions of hydrated electrons, hydrogen atoms and hydroxyl radicals ($^{\bullet}\text{OH}/^{\bullet}\text{O}^{\bullet}$) in aqueous solution, *J. Phys. Chem. Ref. Data* 17 (1988) 513–886.
- [28] S.P. Zhang, S.P. Qian, J.Q. Zhao, S.D. Yao, L.J. Jiang, Characterization of the transient species generated by the photoexcitation of C-phycoerythrin from *Spirulina platensis*: a laser photolysis and pulse radiolysis study, *Biochim. Biophys. Acta* 1472 (1999) 270–278.
- [29] G. Bucher, C.Y. Lu, W. Sander, The photochemistry of lipoic acid: photoionization and observation of a triplet excited state of a disulfide, *ChemPhysChem* 6 (2005) 2607–2618.
- [30] K. Bernhard, J. Geimer, M. Canle-Lopez, J. Reynisson, D. Beckert, R. Gleiter, S. Steenken, Photo- and radiation-chemical formation and electrophilic and electron transfer reactivities of enolether radical cations in aqueous solution, *Chem. Eur. J.* 7 (2001) 4640–4650.
- [31] L. Jian, W.F. Wang, Z.D. Zheng, S.D. Yao, J.S. Zhang, N.Y. Lin, Reactive intermediates in laser photolysis of guanosine, *Res. Chem. Intermed.* 15 (1991) 293–301.
- [32] K.L. Ivanov, E.M. Glebov, V.F. Plyusnin, Y.V. Ivanov, V.P. Grivin, N.M. Bazhin, Laser flash photolysis of sodium persulfate in aqueous solution with additions of dimethylformamide, *J. Photochem. Photobiol. A: Chem.* 133 (2000) 99–104.
- [33] Y. Tang, R.P. Thorn, R.L. Mauldin, P.H. Wine, Kinetics and spectroscopy of the $\text{SO}_4^{\bullet-}$ radical in aqueous solution, *J. Photochem. Photobiol. A: Chem.* 44 (1988) 243–258.
- [34] G.X. Zhang, S. Kimura, A. Nishiyama, T. Shokoji, M. Rahman, L. Yao, Y. Nagai, Y. Fujisawa, A. Miyatake, Y. Abe, Cardiac oxidative stress in acute and chronic isoproterenol-infused rats, *Cardiovasc. Res.* 65 (2005) 230–238.
- [35] C.M. Arroyo, J.H. Kramer, B.F. Dickens, W.B. Weglicki, Identification of free radicals in myocardial ischemia/reperfusion by spin trapping with nitron DMPO, *FEBS Lett.* 221 (1987) 101–104.
- [36] P. Pacher, J.S. Beckman, L. Liaudet, Nitric oxide and peroxynitrite in health and disease, *Physiol. Rev.* 87 (2007) 316–424.